REGULAR ARTICLE

blood advances

Mn porphyrins as a novel treatment targeting sickle cell NOXs to reverse and prevent acute vaso-occlusion in vivo

Madhan Thamilarasan,[1,2] Rodolfo Estupinan,[1,2] Ines Batinic-Haberle,[3] and Rahima Zennadi[1,2]

[1]Division of Hematology, Duke Comprehensive Sickle Cell Center, [2]Department of Medicine, and [3]Department of Radiation Oncology, Duke Cancer Institute, Duke University School of Medicine, Durham, NC

Key Points

- Mn porphyrins reduce cell adhesion, reverse and prevent vaso-occlusion, and improve sickle mouse survival, likely by blocking NOX activity.
- Mn porphyrins are well tolerated and downregulate endothelial adhesion molecule activation and oxidative damage in SCD.

In sickle cell disease (SCD), adhesion of sickle red blood cells (SSRBCs) and activated leukocytes in inflamed venules affects blood rheology, causing vaso-occlusive manifestations and vital reduction in microvascular blood flow. Recently, we found that NADPH oxidases (NOXs) create a vicious feedback loop within SSRBCs. This positive feedback loop mediates SSRBC adhesion to the endothelium. We show for the first time the therapeutic effectiveness of the redox-active manganese (Mn) porphyrins MnTnBuOE-2-PyP^{5+} (MnBuOE; BMX-001) and MnTE-2-PyP^{5+} (MnE; BMX-010, AEOL10113) to treat established vaso-occlusion in a humanized sickle mouse model of an acute vaso-occlusive crisis using intravital microscopy. These Mn porphyrins can suppress SSRBC NOX activity. Subcutaneous administration of only 1 dose of MnBuOE or MnE at 0.1 to 2 mg/kg after the inflammatory trigger of vaso-occlusion, or simultaneously, reversed and reduced leukocyte and SSRBC adhesion, diminished leukocyte rolling, restored blood flow, and increased survival rate. Furthermore, MnBuOE and MnE administered to sickle mice subcutaneously at 0.1 to 1 mg/kg for 28 days (except on weekends) did not exacerbate anemia, which seemed to be due to downregulation of both SSRBC reactive oxygen species production and exposure of the eryptotic marker phosphatidylserine. In addition, Mn porphyrins ameliorated leukocytosis, venous blood gases, endothelial activation, and organ oxidative damage. Our data suggest that Mn porphyrins, likely by repressing NOX-mediated adhesive function of SSRBCs and activated leukocytes, could represent a novel, safe therapeutic intervention to treat or prevent the establishment of acute pain crises. These NOX-targeted antioxidants merit further assessment in SCD clinical trials.

Introduction

In sickle cell disease (SCD), adhesion of the red blood cell (RBC) carrying hemoglobin S (HbS) to endothelial cells (ECs) has been postulated to play a key role in vessel obstruction.[1-4] Vaso-occlusion impairs blood flow, leading to serious life-threatening complications that include acute painful vaso-occlusive crises, called "pain crises," and irreversible damage affecting most vital organs.[4-9] Oxidative stress is increasingly accepted as a trigger of vaso-occlusive episodes.[10-12] Generation of reactive oxygen species (ROS) in sickle RBCs (SSRBCs) is due to both autoxidation of the unstable HbS and activation of intra-erythrocytic NADPH oxidases (NOXs).[13,14] As such, the ensuing oxidative stress in SSRBCs leads to cell adhesion,[15] endothelial oxidative injury and damage, and RBC membrane rigidity and mechanical instability that may contribute to hemolysis.[16] Plus, ECs[17] and activated leukocytes, mainly neutrophils,[18] constitute an additional source of ROS production.[19]

Submitted 10 February 2020; accepted 28 April 2020; published online 1 June 2020.
DOI 10.1182/bloodadvances.2020001642.

Data-sharing requests may be submitted to the corresponding author (Rahima Zennadi, e-mail: zenna001@mc.duke.edu).

The full-text version of this article contains a data supplement.

ROS have been important targets for antioxidant therapies.[20,21] However, none of the antioxidant strategies has thus far been clinically promising in preventing the unpredictable complications of SCD.[22,23] The redox-active manganese (Mn) porphyrins, low-molecular-weight synthetic nonpeptides commonly known as superoxide dismutase (SOD) mimics, have shown remarkable therapeutic effects in kidney, spinal cord, and brain ischemia/reperfusion injuries,[24-27] diseases that have oxidative stress in common with SCD. Importantly, these cationic compounds are nonimmunogenic and can cross the plasma membrane to act primarily in the intracellular compartment. In addition to their role as scavengers of superoxide dismutation, Mn porphyrins are involved in thiol signaling.[28-30] In SCD, the Mn porphyrins MnTnBuOE-2-PyP^{5+} (MnBuOE; BMX-001) and MnTE-2-PyP^{5+} (MnE; BMX-010, AEOL10113) can suppress SSRBC NOX activation.[15] Because of their ability to undergo intricate interactions with numerous redox-sensitive pathways with very limited side effects in animal models,[31] we hypothesized that MnBuOE and MnE by targeting SSRBC NOXs in vivo can treat acute vaso-occlusive crises in a humanized sickle mouse model of an acute vaso-occlusion. Our studies may lead to rapid establishment of Mn porphyrins as a first and novel NOX-targeted therapeutic agent for acute pain crises in SCD.

Materials and methods

Mice

The Institutional Animal Care and Use Committee and the Committee on the Ethics of Animal Experiments at Duke University approved this animal work. All efforts were made to minimize suffering. The 8 to 12 weeks of age, half female and half male transgenic Townes sickle (TS) mice [B6;129-Hbbtm2(HBG1,HBB*)Tow/Hbbtm3(HBG1,HBB)Tow Hbatm1(HBA)Tow/J] were obtained from colonies originally established by T. Townes at the University of Alabama.[32,33] The murine TS model expresses exclusively human α- and sickle β-globins, mimicking the anemia and vasculopathy associated with human SCD.[34,35]

Window chamber surgery

Dorsal skin-fold window chamber surgery was performed as described in detail previously[36] and in the supplemental Methods.

Animal treatments and fluorescence intravital microscopy

In protocol 1 (Figure 1), to reverse an established vaso-occlusion, Mn porphyrin was administered to TS mice after onset of vaso-occlusion triggered by inflammation. Anesthetized animals were injected through a tail vein with 100 μL (0.02% in sterile saline) rhodamine 6G (MilliporeSigma, Burlington, MA) and 0.25 μg/g body weight phycoerythrin-conjugated anti-mouse TER119 (Ly-76) monoclonal antibody (BioLegend, San Diego, CA) for in vivo labeling and monitoring of leukocytes and RBCs, respectively. After 30 minutes, TS mice were injected intraperitoneally with 500 ng murine recombinant tumor necrosis-α (TNF-α) to precipitate vaso-occlusion. Ninety minutes later, a single dose of vehicle (saline) or Mn porphyrin (MnBuOE at 0.1, 0.2, or 2 mg/kg or MnE at 0.5 or 2 mg/kg) was injected subcutaneously. Intravital microscopy was performed before and after drug administration. At least 20 venules of each mouse were recorded.

In protocol 2 (Figure 1), Mn porphyrin was administered to TS mice simultaneously with TNF-α to determine whether the compound can treat an acute vaso-occlusive crisis when it begins. Anesthetized animals with window chamber implants were injected with fluorescent dyes to label leukocytes and RBCs in vivo (as described earlier). Thirty minutes later, animals were injected subcutaneously with 1 dose of vehicle or MnE at 0.5 mg/kg simultaneously with 500 ng TNF-α to initiate vaso-occlusion. Intravital microscopy was performed 90 minutes later and once vaso-occlusion developed. MnBuOE and MnE were synthesized as reported.[37,38]

Cell adhesion was quantified as follows: (1) counting the number of adherent cells/100 μm vessel lengths, by analysis of frame-by-frame video replay using Icy bioimage analysis software (http://icy.bioimageanalysis.org/); and (2) measuring the fluorescence intensity (presented as fluorescence units) of adherent fluorescence-labeled cells on still images (20×) using ImageJ software downloaded from the National Institutes of Health Web site. Rolling flux was determined by counting the number of leukocytes rolling through a given point in a vessel (number of leukocytes per minute) via frame-by-frame analysis of video replay using Icy bioimage analysis software. The values obtained from analyzing all recorded vessel segments were averaged among groups of animals for statistical analysis. The percentages of vessels with normal blood flow, slow blood flow, and occluded vessels were calculated by dividing the number of each: vessels (both small and large) with normal blood flow, slow blood flow, and no blood flow by the total number of vessels recorded in all animals.

RBC ROS detection

ROS detection in RBCs was performed by using CM-H2-DCFDA (DCF; Thermo Fisher Scientific (Waltham, MA), as described previously in detail.[15]

RBC phosphatidylserine exposure

Phosphatidylserine (PS) exposure on isolated RBCs was measured by using green fluorescent protein (GFP)–labeled annexin V binding by flow cytometry. The methods have been described previously in detail.[15]

Complete blood count analysis

To evaluate whether Mn porphyrins are well tolerated, complete blood count (CBC) was determined in peripheral blood collected from nonsedated TS mice injected subcutaneously daily for 28 days, except on weekends, with 1 dose per day of vehicle, 0.1 mg/kg MnBuOE, and 1 mg/kg MnE. CBC was performed by automated determination of the absolute numbers and ratios of various cell types by using a CBC machine (VetScan Hm5C; Abaxis Inc., Union City, CA).

Reticulocyte counts

Blood samples collected from nonsedated TS mice injected subcutaneously daily for 28 days except on weekends with 1 dose per day of vehicle, 0.1 mg/kg MnBuOE, and 1 mg/kg MnE were incubated with 10 mg/mL acridine orange for 30 minutes at room temperature in the dark. Data acquisitions were then performed by using flow cytometric analysis.

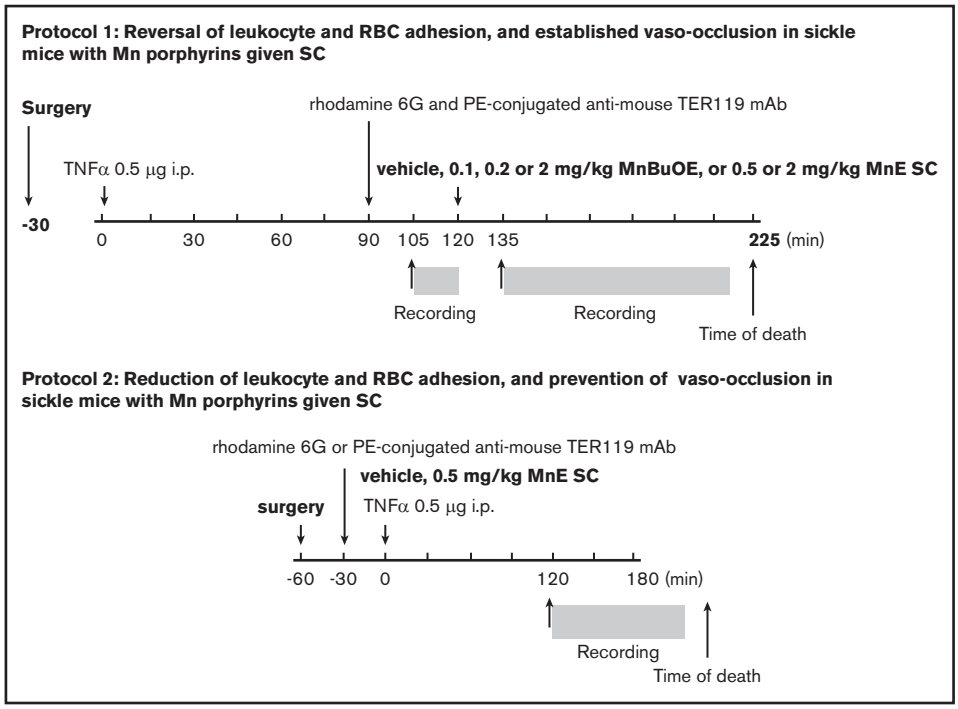

Figure 1. Schematic representation of intravital microscopy protocols. Protocol 1 was designed to assess the action of MnBuOE and MnE on ongoing acute vaso-occlusive crises triggered by inflammation in TS mice. Anesthetized TS mice with window chamber implants were injected subcutaneously (SC) with 0.1, 0.2, or 2 mg/kg MnBuOE, 0.5 mg/kg or 2 mg/kg MnE, or vehicle (saline) 120 minutes after TNF-α challenge (time 0). Fifteen minutes before and 15 minutes after drug injection, blood cell behavior in the subdermal vasculature was recorded between the time points of 105 and 120 minutes ($T_{105} \rightarrow T_{120}$) and 135 and 225 minutes ($T_{135} \rightarrow T_{225}$), respectively. Protocol 2 was designed to assess the action of MnE on preventing precipitation of vaso-occlusion when given simultaneously with TNF-α, the inflammatory trigger of vaso-occlusion in TS mice. Anesthetized TS mice with window chamber implants were injected first with dyes for in vivo fluorescence cell labeling as described in "Materials and methods." Thirty minutes after cell labeling, mice were SC administered 1 dose of 0.5 mg/kg MnE, or vehicle (saline), then challenged immediately with TNF-α (time 0). After 120 minutes, intravital microscopy was performed, and blood cell behavior in the subdermal vasculature was recorded between the time points of 120 and 180 minutes ($T_{120} \rightarrow T_{180}$). i.p., intraperitoneally; mAb, monoclonal antibody; PE, phycoerythrin.

Venous blood gas analysis

Venous blood gases in peripheral blood collected from nonsedated TS mice injected subcutaneously daily for 28 days except on weekends with vehicle, 0.1 mg/kg MnBuOE, and 1 mg/kg MnE were analyzed. Analysis was conducted by using a VetScan i-STAT portable bio-analyzer (Abaxis, Inc.) and CG4$^+$ single-use cartridges that can measure different analytes: pH, partial carbon dioxide pressure (pCO_2), partial oxygen pressure (pO_2), base excess of the extracellular fluid (BEecf), bicarbonate (HCO_3^-), total carbon dioxide (TCO_2), hemoglobin saturation of oxygen (sO_2), and lactate.

Organ collection, endothelial ROS, and tissue apoptosis

Lungs, kidneys, liver, and spleen harvested from euthanized animals were processed as described elsewhere.[36] Kidney, liver, and spleen tissue sections of 10 μm thickness were stained with DCF for ROS detection, or double-stained with GFP-conjugated annexin V and propidium iodide (PI) (BioLegend) for apoptosis as recommended by the manufacturer. After staining, washed tissue sections were fixed with 2% formaldehyde. Tissue sections were then examined by using inverted fluorescence microscopy (Carl Zeiss AG, Oberkochen, Germany). Five random fields were imaged for each section of each organ, and fluorescence intensity for each field was quantified by using ImageJ software. The values were averaged for the 5 fields and among groups of animals for statistical analysis.

Endothelial adhesion molecule expression by quantitative real-time polymerase chain reaction

Total RNA was isolated from the lungs, kidneys, liver, and spleen by using TRIzol reagent (Ambion, Foster City, CA) according to the manufacturer. Complementary DNAs were prepared by using SuperScript III First-Strand Synthesis kit (Thermo Fisher Scientific). Relative expression of VCAM-1, ICAM-1, and P-selectin messenger RNAs (mRNAs) was measured and then normalized to an endogenous control 36B4 (Rplp0) gene. Sequences of primers used to assess gene expression are described in the supplemental Methods.

Western blot

Tissue samples were homogenized, and protein separation was performed by using polyacrylamide gel electrophoresis with 20 μg proteins per lane. Western blots using the appropriate antibodies were performed.[39] Bands were analyzed densitometrically by using ImageJ software. Protein expression data were normalized according to GAPDH (glyceraldehyde-3-phosphate dehydrogenase) expression.

Statistical analysis

Data were compared by using parametric analyses (Prism 5 software; GraphPad Software, San Diego, CA), including repeated and nonrepeated measures of analysis of variance. One- and 2-way analyses of variance were followed by Bonferroni corrections for multiple comparisons (multiplying the P value by the number of comparisons). $P < .05$ was considered significant.

Results

Mn porphyrins reverse cell adhesion after the inflammatory trigger of vaso-occlusion in sickle mice in vivo

Human sickle cell pain crises are associated with inflammation.[40] Vaso-occlusion in sickle mice can be precipitated by administering TNF-α, a proinflammatory cytokine. Other investigators have discovered that sickle mice are highly susceptible to systemic inflammation.[41] Indeed, injecting TNF-α into these mice before the surgical preparation led to animal death during or soon after the surgical insult as opposed to control animals and sickle mice that did not receive TNF-α. Thus, because the surgical preparation of the dorsal skin-fold window chamber implant itself initiates an inflammatory response, our rationale was to monitor cell behavior in the microcirculation of sickle mice during inflammation induced by surgical insult and then augmented by TNF-α administration. To accurately evaluate the therapeutic benefits of Mn porphyrins to treat an acute vaso-occlusive crisis triggered by TNF-α, intravital microscopy was performed before and after drug administration.

We investigated the effect of MnBuOE and MnE on cell adhesion in TS mice 135 minutes after TNF-α administration (Figure 1), a time at which leukocytes have already been recruited and adhered, SSRBCs are bound to adherent leukocytes and the endothelium, and vaso-occlusive–like processes are observed in the microvessels. Because only occasional SSRBCs interact with ECs and adherent leukocytes in sickle mice after TNF-α challenge, cell adhesion consisted of adhesion of both fluorescence-labeled SSRBCs and fluorescence-labeled leukocytes. Intravital microscopy performed before drug administration (prior to treatment) showed avid cell adhesion in inflamed vessels of TS mice, promoting occlusion of some venule segments with apparent blood stasis (Figure 2A-E). Cell adhesion and vaso-occlusion were not affected by vehicle treatment; vessel occlusion was intermittent and transient, and lasted in some of the vessels up to 223 minutes following TNF-α injection ($P > .05$) (supplemental Video 1). Conversely, cell adhesion and vaso-occlusion were reversed dose dependently following subcutaneous injection to animals of only 1 dose of 0.1, 0.2, and 2 mg/kg MnBuOE compared with vehicle therapy (supplemental Video 2). The number of adherent cells over 100-μm venular lengths was reduced by 68% ± 4% ($P < .05$), 85% ± 2.3% ($P < .01$), and 89% ± 4% ($P < .01$) following 0.1, 0.2, and 2 mg/kg MnBuOE treatments, respectively (Figure 2B). Fluorescence intensities of adherent fluorescence-labeled cells were also diminished by 64% ($P < .05$), 66% ($P < .01$), and 66% ($P < .01$) with 0.1, 0.2, and 2 mg/kg MnBuOE (Figure 2C).

Similarly, 60 minutes later, SSRBC and leukocyte adhesion in inflamed vessels and vaso-occlusion were reversed dose dependently by 0.5 and 2 mg/kg MnE (Figure 2A-E; supplemental Video 3), and the number of adherent cells was decreased by 76% ± 8.6% and 91% ± 2.5%, respectively, compared with vehicle or before treatment (Figure 2B). Fluorescence intensities of adherent cells were comparatively diminished (99% reduction) in animals treated with 0.5 and 2 mg/kg MnE (Figure 2C). The effect of Mn porphyrins was sustained over time.

Rolling of leukocytes (which can be distinguished from RBCs based on their morphology) along the postcapillary vessels is a prerequisite step, and it occurs before leukocyte adhesion to the vessel wall and subsequent leukocyte extravasation.[42,43] Intravital microscopy revealed high numbers of rolling leukocytes (an average of 57 leukocytes rolling per minute) in TS mice before treatment (Figure 2D), which were sustained after treatment with vehicle (an average of 51 leukocytes rolling per minute). However, the numbers of rolling leukocytes declined over time by 49% ($P > .05$), 69% ($P < .01$), 88% ($P < .001$), 69% ($P < .01$), and 75% ($P = .0031$) following treatments with 0.1, 0.2, and 2 mg/kg MnBuOE and 0.5 and 2 mg/kg MnE, respectively, compared with vehicle treatment.

Reversal of cell adhesion and lowered leukocyte rolling by 0.1, 0.2, and 2 mg/kg MnBuOE, and 0.5 and 2 mg/kg MnE led to reestablishment of blood flow in 64%, 74%, 78%, 79%, and 89% of the total vessels recorded, respectively, compared with only 32% of the venules with normal blood flow in the vehicle group (Figure 2E).

TNF-α–induced vaso-occlusion in sickle mice could lead to death within several hours. TS mice were therefore monitored for >72 hours after the TNF-α challenge to assess the effect of the Mn porphyrin therapy on mortality under a crisis condition. Kaplan-Meier survival curves showed prolonged survival of TS mice treated with 2 mg/kg MnE under TNF-α–induced crisis conditions compared with vehicle control (log-rank test, $P = .0009$) (Figure 2F). The median survival in vehicle-treated control mice was at least 17 hours shorter than in MnE-treated TS mice (11.08 hours vs 28 hours, respectively, after TNF-α injection). Taken together, these results strongly argue that subcutaneous Mn porphyrin therapy may be beneficial in SCD during an acute crisis, by at least negatively regulating RBC and leukocyte adhesive functions.

Mn porphyrins diminish SSRBC ROS levels triggered by inflammation in sickle mice

We investigated whether reversal of vaso-occlusion by Mn porphyrins is due to reduction in SSRBC NOX-dependent ROS production.[15] Treatments of TS mice with 1 dose of MnBuOE at 0.1, 0.2, and 2 mg/kg and MnE at 0.5 and 2 mg/kg significantly decreased SSRBC ROS levels compared with vehicle treatment ($P < .05$ for MnBuOE and MnE treatments) (Figure 2G), suggesting that Mn porphyrins reduce SSRBC ROS generation in vivo most likely by suppressing SSRBC NOX enzymes, as we have shown previously.[15]

Mn porphyrins reduce establishment of vaso-occlusion triggered by inflammation and improve blood stasis by inhibiting SSRBC and activated leukocyte adhesive function in sickle mice

The effect of Mn porphyrin on preventing the establishment of an acute painful vaso-occlusive crisis triggered by TNF-α in TS mice was assessed. Intravital microscopy observations of the microvasculature of animals injected subcutaneously with only 1 dose of

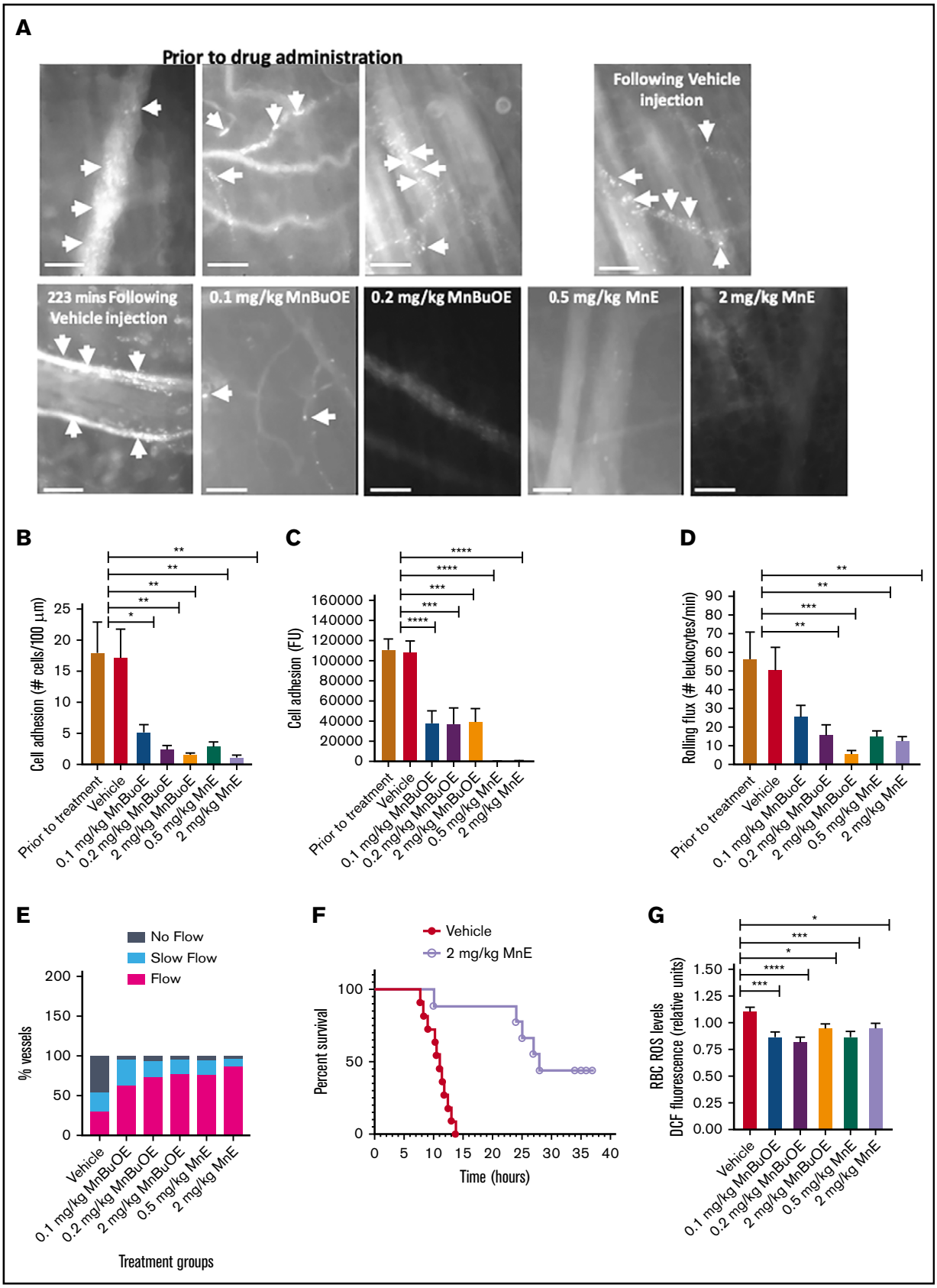

Figure 2. Mn porphyrin administration to TS mice after the inflammatory challenge reverses cell adhesion and leukocyte recruitment, and it restores blood flow by reducing SSRBC ROS production. Anesthetized TS mice were treated subcutaneously with vehicle, 0.1, 0.2, or 2 mg/kg MnBuOE, or 0.5 mg/kg or 2 mg/kg MnE,

vehicle in chorus with TNF-α showed extensive activated leukocyte and SSRBC interactions with inflamed vessels (Figure 3A-D), obstructing blood venules as reflected by blood stasis (Figure 3E). In sharp contrast, MnE at 0.5 mg/kg administered simultaneously with TNF-α had an anti-leukocyte and anti-SSRBC adhesive activity ($P < .01$), diminishing the number of adherent cells by 62% ($P < .01$) compared with vehicle treatment (Figure 3B). Reproducible results were obtained when adhesion of fluorescence-labeled cells was quantitated (Figure 3C). MnE at 0.5 mg/kg lowered the number of rolling leukocytes by 74% as well ($P < .01$) (Figure 3D). As a result of inhibition of cell adhesion, normal blood flow was preserved in 74% of the total vessels recorded in the group treated with 0.5 mg/kg MnE (Figure 3E). Only 26% of the total vessels recorded showed slow-moving blood flow in MnE-treated animals, as opposed to 11% and 47% of the total microvessels recorded with blood stasis and sluggish blood flow, respectively, in vehicle-treated TS mice. These data suggest that Mn porphyrin can prevent inflammation from establishing and/or exacerbating vaso-occlusion, when the compound is given just before or as soon as an acute crisis begins.

Mn porphyrins are well tolerated by sickle mice and alleviate leukocytosis

To determine whether Mn porphyrins are well tolerated by TS mice, we first evaluated the effect of Mn porphyrins on the apoptosis-like RBC death called eryptosis, which is characterized by cell shrinkage and PS externalization. TS mice were treated subcutaneously for 4 weeks except on weekends with 1 dose per day of Mn porphyrin. TS mice treated with vehicle exhibited 4.98% ± 0.6% annexin V–positive SSRBCs (Figure 4A). However, 0.1 mg/kg MnBuOE and 1 mg/kg MnE markedly decreased the percentage of annexin V–binding SSRBCs by 54% ($P = .0009$) and 56% ($P = .0007$), respectively. We next assessed the effect of the compounds on RBC counts; as a result of improved eryptosis, RBC counts rose from 5.23 × 10^6/μL in vehicle-treated mice to 5.99 × 10^6/μL in MnE-treated mice (Table 1). Similarly, hemoglobin levels rose from 7 g/dL in vehicle-treated TS mice to 8.55 g/dL after MnE treatment. In concordance with these findings, hematocrits rose from 26.1% in vehicle-treated mice to 28.59% in MnE-treated mice, without substantially affecting reticulocyte counts, implying less hemolysis and no increase in RBC production.

In addition, prolonged treatments of TS mice with 0.1 mg/kg MnBuOE and 1 mg/kg MnE significantly reduced the SSRBC ROS production profile compared with SSRBC ROS levels in vehicle-treated mice ($P < .05$) (Figure 4B). This finding suggests that Mn porphyrins protect SSRBCs especially against NOX activation.

Leukocytosis in SCD is associated with increases in the incidence of pain crisis, acute chest syndrome, stroke, and mortality.[44] Studies have reported increased inflammation and leukocyte counts, including neutrophils in patients and transgenic murine models of SCD.[44-47] We further evaluated the effect of Mn porphyrins on leukocytosis in sickle mice. Twenty-eight-day dosing of TS mice with 0.1 mg/kg MnBuOE and 1 mg/kg MnE significantly decreased leukocyte counts, which became close to or within the normal range (6 × 10^3 to 15 × 10^3/μL) (Figure 4C). Neutrophil (Figure 4D) and lymphocyte (Figure 4E) counts became normal (0.5 × 10^3 to 3.8 × 10^3/μL and 3.46 × 10^3 to 7.44 x 10^3/μL, respectively) after MnBuOE and MnE therapies. Monocyte counts were also significantly reduced by MnE ($P < .05$) (normal ranges, 0 to 0.6 × 10^3/μL) (Figure 4F). Together, these data suggest that Mn porphyrins are well tolerated by sickle mice, can alleviate leukocytosis, and may ameliorate inflammation in SCD.

Mn porphyrins can improve venous blood gases in sickle mice

Venous blood gases can provide information on acid-base status and ventilation, and may be affected by oxidative stress. Blood was collected from 28-day dosing with vehicle of TS mice that had not been sedated before and during blood withdrawal; the samples showed impaired venous blood gases with a pH varying from 7.1 to 7.5 (normal ranges, 7.31-7.41) (Figure 5A) and levels of pCO_2 (Figure 5B), pO_2 (Figure 5C), BEecf (Figure 5D), HCO_3^- (Figure 5E), TCO_2 (Figure 5F), and sO_2 (Figure 5G) below normal, and lactate levels (Figure 5H) above normal, levels compatible with hyperventilation. However, 28-day dosing of TS mice with 0.1 mg/kg MnBuOE showed a trend toward ameliorating pH, pCO_2, pO_2, BEecf, HCO_3^-, TCO_2, and sO_2, and a significant decrease in lactate. MnE at 1 mg/kg alternatively had a much better effect than MnBuOE on pH (varying from 7.172 to 7.406); significantly increased pCO_2, pO_2, BEecf, HCO_3^-, TCO_2, and sO_2; and decreased lactate levels ($P < .05$). These data suggest that Mn porphyrins may improve acid-base status and ventilation in SCD.

Mn porphyrins downregulate organ ROS production and endothelial activation in sickle mice

We next assessed whether Mn porphyrins affect ROS production and expression of the adhesion molecules VCAM-1, ICAM-1, and P-selectin (markers of endothelial dysfunction and disease severity,[48-50], and/or RBC and leukocyte adhesion in SCD)[51-54];

Figure 2. (continued) as per protocol 1. (A) Representative images of postcapillary venules (20× magnification) from vehicle-treated and compound-treated TS mice are presented. Vessels without adherent cells appear gray due to the rapidly moving fluorescence-labeled cells. Sickle RBC and leukocyte adhesion in inflamed vessels and vaso-occlusion are indicated with arrows. Scale bars, 50 μm. (B-D) Video frames of vessel and arteriole segments were used to quantify adhesion of fluorescence-labeled cells (sickle RBCs and leukocytes) presented as the number of adherent cells per 100 μm vessel length and fluorescence unit [FU], and rolling flux of leukocytes. The number of leukocytes (identified based on their size) rolling across a specific point per minute was counted. At least 50 different locations were analyzed for rolling of leukocytes in the vessels, and numbers were averaged among groups of TS mice. (A-C) Before and after treatment with vehicle, TS mice showed marked cell adhesion and vaso-occlusion. Treatment with 0.1, 0.2, or 2 mg/kg MnBuOE or 0.5 or 2 mg/kg MnE reversed cell adhesion and vaso-occlusion. (E) Blood flow in TS mice. Percentage of vessels with normal, slow, and no blood flow in vessels with a venular diameter almost similar (~25 μm) among all groups tested. (F) The Kaplan-Meier survival curves for MnE-treated (n = 9) or vehicle-treated (n = 11) TS mice. Survival was significantly improved in the MnE-treated group compared with vehicle control. Log-rank (Mantel-Cox) test, $P = .0009$. (G) ROS generation in sickle RBCs in vivo. Compared with vehicle treatment, TS mice treated with MnBuOE at 0.1, 0.2, and 2 mg/kg and MnE at 0.5 and 2 mg/kg manifest significantly lower SSRBC ROS measurements of DCF-derived signal. (B-D,G) Error bars show standard error of the mean (SEM) of 4 different experiments for each treatment group. *$P < .05$, **$P < .01$, ***$P < .001$, and ****$P < .0001$ compared with vehicle-treated animals regardless of the vessel diameter.

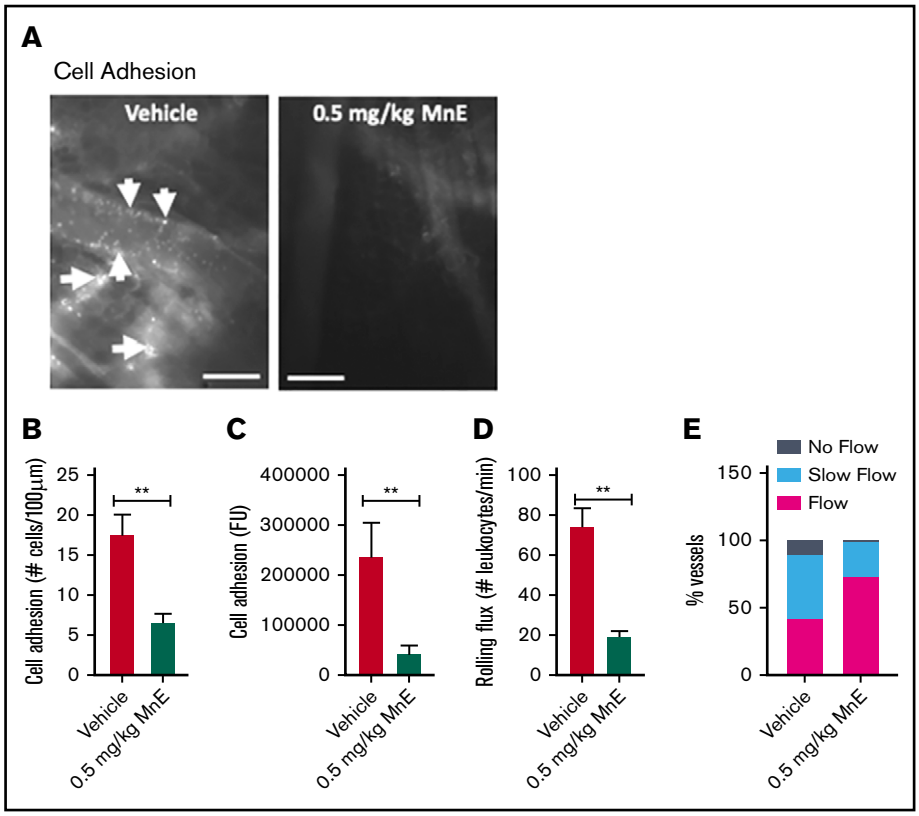

Figure 3. Mn porphyrins reduce cell adhesion and restore blood flow in vivo. (A-E) TS mice were treated subcutaneously with 1 dose of vehicle or 0.5 mg/kg MnE, followed immediately by 500 ng TNF-α; intravital microscopy was then performed per protocol 2. (A) Intravital microscopy was performed on anesthetized treated TS mice. Representative images of postcapillary venules (20× magnification) from treated TS mice are presented. Leukocyte and RBC adhesion and vaso-occlusion are indicated with arrows. Scale bars, 50 μm. (B-D) Video frames showing vessel segments were used to quantify fluorescence-labeled cell (leukocyte and RBC) adhesion (B-C) and leukocyte rolling flux (D) in all venules and arterioles were recorded, and numbers were averaged among groups of animals. Cell adhesion presented as number of adherent cells per 100 μm vessel length (B), and fluorescence unit (FU) (C). Leukocyte rolling flux presented as number of leukocytes per minute (D). TS mice injected simultaneously with 1 dose of 0.5 mg/kg MnE and TNF-α showed sporadic cell adhesion (B-C) and reduced leukocyte rolling (D) as opposed to the vehicle group. (E) Blood flow in vivo. Percentage of vessels with normal, slow, and no blood flow (occluded vessels) are shown. Average vessel diameter was almost identical (~21 μm) in all treatment groups. Blood stasis in TS mice treated with 0.5 mg/kg MnE was significantly reduced compared with the vehicle group. Error bars show SEM of 6 different experiments for each treatment group. **$P < .01$ compared with vehicle treatment regardless of the vessel diameter within the ranges specified.

we used tissue sections of the kidneys, liver, spleen, and the lungs, organs typically impaired in SCD.[10,55] MnBuOE at 0.1 mg/kg and MnE at 1 mg/kg significantly decreased ROS levels in the kidneys ($P < .03$ for MnBuOE and MnE), liver ($P < .05$ for MnBuOE and MnE), and spleen ($P < .004$ for MnBuOE and MnE) compared with the vehicle group (Figure 6A-C).

MnBuOE at 0.1 mg/kg suppressed ICAM-1 and VCAM-1 mRNA levels in the lungs ($P < .0001$ and $P = .0054$, respectively) and kidneys ($P = .0072$ and $P = .0004$), and P-selectin mRNA expression ($P = .0058$) in the kidneys (Figure 6D-F). MnE at 1 mg/kg downregulated the levels of ICAM-1 mRNA in the lungs ($P < .0001$) and kidneys ($P = .0125$), and VCAM-1 mRNA ($P = .0038$) in the kidneys. However, ICAM-1, VCAM-1, and P-selectin mRNA levels in the liver and spleen were not affected by these compounds. Protein expression levels of VCAM-1 analyzed by western blots also decreased in the lungs ($P < .05$) and kidneys ($P < .01$), as well as ICAM-1 ($P < .01$) and P-selectin ($P < .01$) in the kidneys after MnBuOE treatment of sickle mice (Figure 6G-J). Similarly, MnE treatment of sickle mice reduced protein expression levels of VCAM-1 in the lungs ($P < .01$) and kidneys ($P < .05$), and ICAM-1 ($P < .05$) but not P-selectin, in the kidneys. In contrast, no real changes were detected in protein expression levels of these adhesion molecules in the spleen and liver between the different treatment groups (data not shown). Together, these data suggest that reduced endothelial ROS content by these compounds could consequently downregulate VCAM-1, and/or ICAM-1 and P-selectin activation, especially in the kidneys and to a less extent the lungs in SCD, and further confirm the safety of Mn porphyrins.

Mn porphyrins alleviate tissue apoptosis

We further assessed the effect of Mn porphyrins on organ damage in SCD. Vehicle-treated TS mice for 28 days showed marked apoptosis (double-staining with GFP-labeled annexin V and PI) in the kidney, liver, and spleen tissues (Figure 7A) and reflected by the fluorescence intensity of GFP-labeled annexin V binding and PI staining quantitated separately (Figure 7B-G). However, 0.1 mg/kg MnBuOE significantly reduced apoptosis in the kidneys ($P < .0001$) (Figure 7A-C), liver ($P < .05$) (Figure 7A,D,E), and spleen ($P < .05$) (Figure 7A,F,G) compared with the vehicle group.

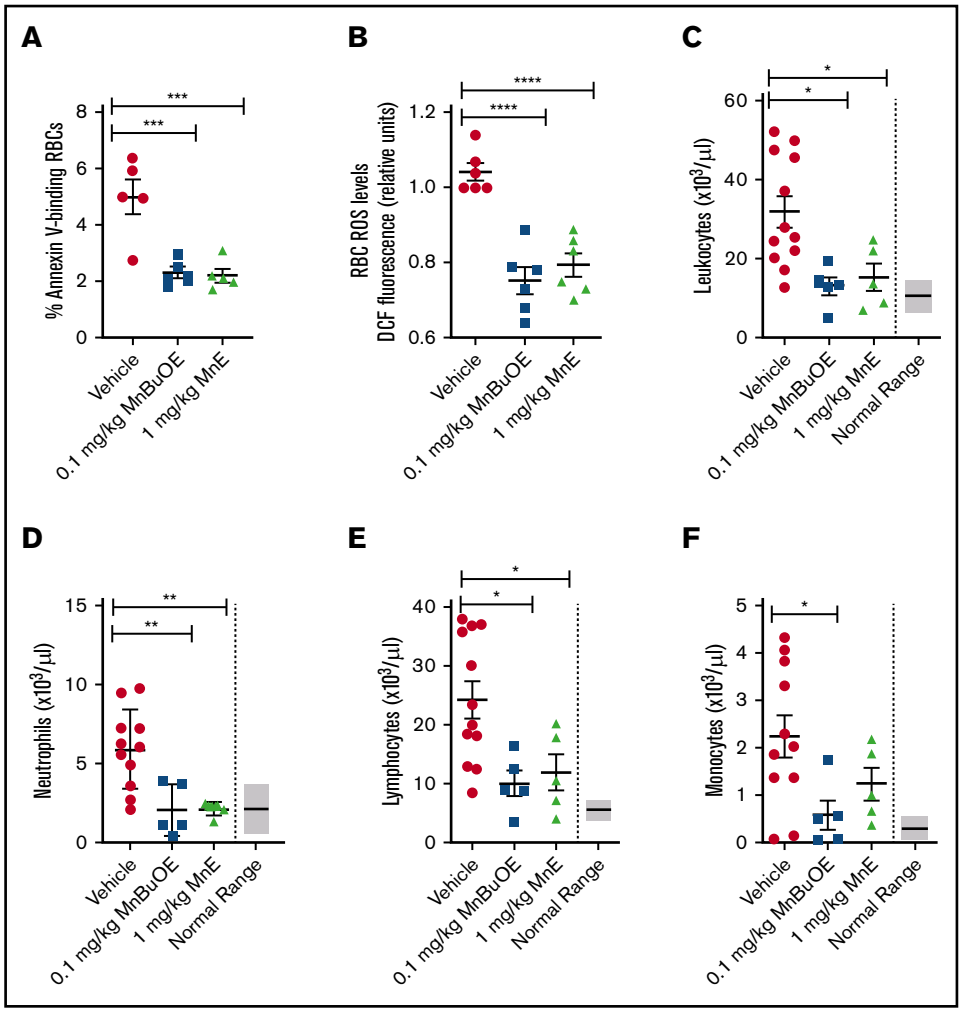

Figure 4. Mn porphyrins reduce eryptosis, SSRBC oxidative stress, and leukocytosis in TS mice in vivo. TS mice were dosed daily for 28 days except on weekends with 1 dose per day of vehicle, 0.1 mg/kg MnBuOE, and 1 mg/kg MnE injected subcutaneously. (A) PS exposure of sickle RBCs in treated TS mice. Dynamics of RBC PS exposure analyzed with GFP-labeled annexin V on Mn porphyrin-improved eryptosis in TS mice. The data presented as SEM of 5 different experiments per treatment group. ***$P < .001$ vs vehicle. (B) SSRBC ROS production in treated TS mice. SSRBCs isolated from blood of treated TS mice were tested for the levels of ROS using DCF as an indicator of ROS in cells. MnBuOE and MnE significantly decreased ROS production in sickle RBCs compared with vehicle treatment. Error bars show SEM of 6 different experiments per treatment group. ****$P < .0001$ vs vehicle. (C-F) Leukocytosis evaluation in treated sickle mice. Blood drawn through the submandibular vein was assessed for complete blood count. Total leukocyte (C), neutrophil (D), lymphocyte (E), and monocyte (F) counts are shown. Data are presented as SEM. *$P < .05$ and **$P < .01$ compared with vehicle controls.

Similarly, 1 mg/kg MnE significantly relieved the kidney ($P = .0001$) and liver ($P < .007$) tissue apoptosis compared with the vehicle treatment but without affecting the spleen. These data suggest that tissue oxidative stress reduction by Mn porphyrins can at least alleviate organ damage.

Discussion

Redox homeostasis plays a pivotal role in precipitating and/or exacerbating vaso-occlusion in SCD. Numerous studies have attempted to reduce endothelial oxidative stress, thus enhancing antioxidant defenses in sickle mice to prevent adhesion of leukocytes[10,56] and RBCs[11] and vaso-occlusion in vivo using polynitroxyl albumin,[10,11] allopurinol,[56] an inhibitor of xanthine oxidase (XO),[11,56] and dimethyl fumarate,[12] the activator of nuclear factor erythroid-2–related factor-2 (Nrf2), which is a regulator of cellular cytoprotective responses to heme, iron, and oxidative stress. However, thus far, there are no data regarding targeting NOX-dependent ROS production in SSRBCs and/or the endothelium and leukocytes to primarily reverse established vaso-occlusion. Our in vivo data now reveal a promising NOX-targeted therapy with the redox-active Mn porphyrins that can be administered subcutaneously in SCD, a therapy that not only inhibits vaso-occlusion from being established but, above all, reverses ongoing vaso-occlusion, leading to improved survival.

Treatment of sickle mice with only 1 dose of the Mn porphyrins MnBuOE and MnE effectively reversed adhesion of sickle RBCs and leukocytes in inflamed venules, leukocyte rolling along the venular walls, and vaso-occlusion, resulting in reestablishment of

Table 1. Mn porphyrins do not exacerbate hemolysis

Treatment	RBCs, $\times 10^6/\mu L$	Hemoglobin, g/dL	Hematocrit, %	Reticulocytes, %
Vehicle	5.23 ± 0.67	7 ± 0.86	26.12 ± 1.75	52.2 ± 3.61
1 mg/kg MnE	5.99 ± 0.96	8.55 ± 0.97	28.59 ± 1.1	50.41 ± 0.48

TS mice (n = 4/group) were treated subcutaneously with vehicle or 1 mg/kg MnE daily for 28 days except on weekends. After 28 days of treatment, venous blood was collected, and complete blood counts were measured. Data are presented as the mean ± SEM.

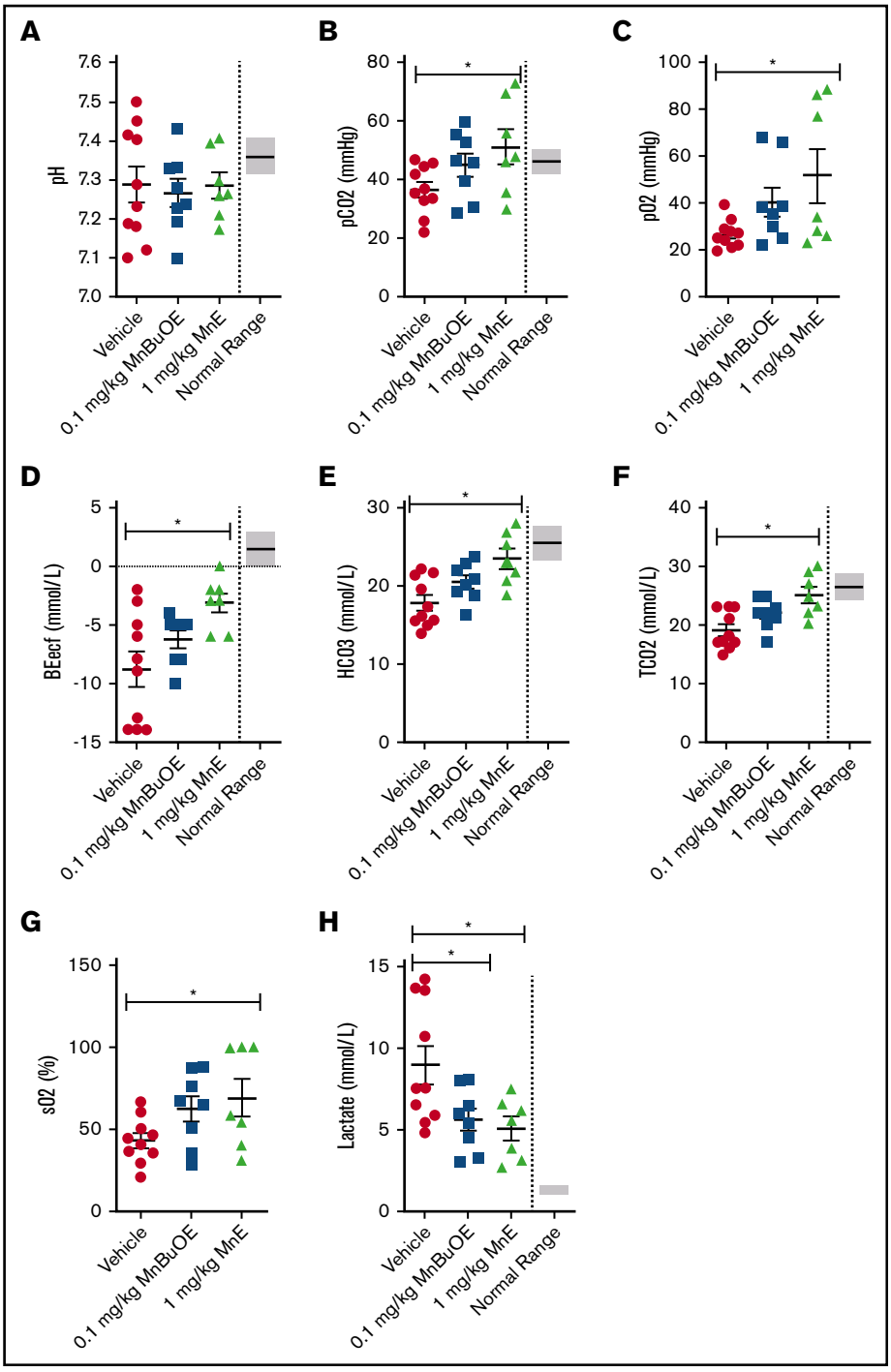

Figure 5. Mn porphyrins can ameliorate venous blood gases in TS mice in vivo. TS mice were treated for 28 days, except on weekends, with 1 subcutaneous dose per day of vehicle (n = 10), 0.1 mg/kg MnBuOE (n = 8), or 1 mg/kg MnE (n = 7). i-STAT analysis of the collected blood revealed that venous blood gases could be improved by Mn porphyrins. (A) pH values were somewhat affected with the Mn porphyrins. The levels of pCO_2 (B), pO_2 (C), BEecf (D), HCO_3^- (E), TCO2 (F), and sO_2 (G) increased to some degree in TS mice treated with 0.1 mg/kg MnBuOE and became close to or within the normal ranges in mice treated with 1 mg/kg MnE. (H) Lactate levels significantly decreased in TS mice treated with 0.1 mg/kg MnBuOE and 1 mg/kg MnE. Data are presented as SEM. *$P < .05$ compared with vehicle treatment.

blood flow and amelioration of the survival rate. Reversal of SSRBC and leukocyte adhesion and vaso-occlusion by MnBuOE and MnE was due at least in part to suppression of excessive ROS production in SSRBCs, and likely the endothelium and leukocytes. Mn porphyrins equally hindered establishment and/or progression of a vaso-occlusive process when given as soon as an inflammatory insult occurred in vivo by diminishing adhesion of SSRBCs and leukocytes in inflamed venules and leukocyte rolling, subsequently ameliorating blood flow. We recently reported that MnBuOE and MnE inhibit human SSRBC ROS production-mediating adhesion via NOX suppression.[15] Neutrophils in particular also have an important role in vaso-occlusion by interacting with the endothelium and sickle RBCs; NOXs in activated leukocytes are a major source of ROS production as well.[41,57] In addition, evidence has involved endothelial NOX-derived superoxide in the adhesion of leukocytes and platelets in cerebral venules of sickle mice.[17] Thus, NOXs/ROS in SSRBCs, and possibly in ECs and leukocytes, seem to be one of the major driving forces behind an acute vaso-occlusive event in SCD. Therefore, in addition to the effect of Mn porphyrins on sickle RBCs, these compounds may reduce leukocyte adhesive activity

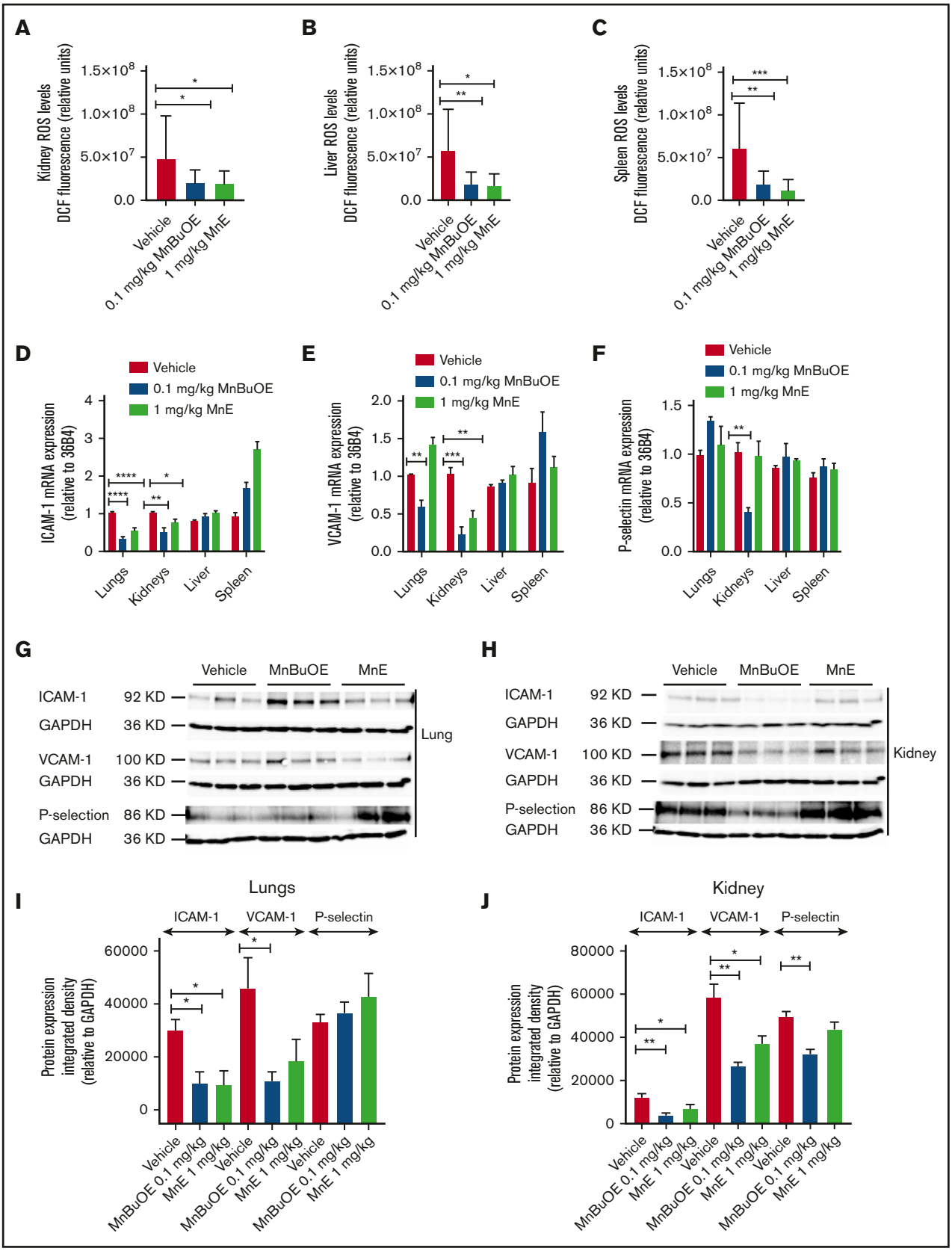

Figure 6. Mn porphyrins alleviate RBC and tissue oxidative stress, and endothelial activation in TS mice in vivo. TS mice were dosed subcutaneously daily for 28 days except on weekends with 1 dose per day of vehicle, 0.1 mg/kg MnBuOE, and 1 mg/kg MnE. (A-C) Quantitative analysis of images of tissue organs (n = 5 random

and endothelial dysfunction by possibly at least inhibiting endogenous NOX-dependent ROS production. NOXs, the major superoxide-producing enzymes, are a potentially noteworthy source of ROS in SCD, especially because in this disorder the absolute involvement of soluble circulating XO and endothelial-associated XO in ROS formation in the microvasculature remains unclear. XO activation seems to be tissue specific because some tissues (eg, the brain) exhibit little or no XO activity, whereas other tissues (eg, intestine) display high XO activity.

Mn porphyrins were well tolerated by sickle mice, as evidenced by improved eryptosis reflected at least in part by reduced RBC PS exposure, and subsequently hemolysis. Also, although potential external and/or internal confounders could interfere with venous blood gases, these parameters, especially hemoglobin saturation of oxygen and lactate (the indicator of hypoxia), were restored to some extent by the Mn porphyrins. Bettering eryptosis and venous blood gases in sickle mice by Mn porphyrins seems to be due partially to the marked decrease in sickle RBC ROS produced in excess and oxidative stress. The safety of the Mn porphyrins in sickle mice could also result from the ability of these agents to alleviate leukocytosis, by reducing all, neutrophil, monocyte, and lymphocyte counts, possibly through inhibition of NOX-dependent ROS generation. We speculate that reduced leukocyte counts are possibly due to the ability of Mn porphyrins to decrease inflammatory markers,[58,59] as proinflammatory cytokines can increase myelopoiesis.[60,61] Neutrophils are in an activated state in SCD, and high baseline leukocyte numbers are associated with increased morbidity and mortality in SCD.[44]

Furthermore, the substantial levels of oxidative stress in SSRBCs enhance HbS autoxidation, which could contribute to cell membrane damage, premature erythrocyte aging, and hemolysis.[16] Extracellular hemoglobin and heme in plasma or microparticles[62] then promote severe oxidative stress, not only to blood cells but also to blood vessels, leading to vascular dysfunction and vaso-occlusion in SCD.[63,64] Increased NOX-dependent ROS generation can signal NF-κB activation in the endothelium, which in turn triggers EC adhesion molecule expression (eg, VCAM-1, ICAM-1, P-selectin [the latter of which can be directly upregulated by ROS]),[10,63] promoting leukocyte recruitment, SSRBC/leukocyte adhesion, transient vaso-occlusion, and ischemia/reperfusion. Free heme in addition stimulates an activated proinflammatory, proadhesive, and prothrombotic phenotype. Furthermore, extracellular hemoglobin scavenges nitric oxide, consequently decreasing nitric oxide bioavailability,[65] which results in vascular dysfunction and vaso-restriction. We suggest that reduced eryptosis and hemolysis by Mn porphyrins, together with the direct or indirect effect of these agents on endothelial damage caused by hemolysis, can lead to alleviation of endothelial oxidative stress by these agents, as shown by decreased ROS generation in multiple organs; ensuing down-regulation of VCAM-1, ICAM-1, and P-selectin expression; and improved endothelial dysfunction and oxidative organ damage in sickle mice.

In addition to their role as powerful SOD mimics, Mn porphyrins as catalysts of superoxide dismutation can rapidly react with a number of other species; it has been suggested that they are involved in thiol signaling,[28-30] catalytically oxidizing protein cysteines in a glutathione peroxidase fashion by using H_2O_2 and glutathione.[28,66,67] Mn porphyrins also modify the activity of transcription factors such as NF-κB and, in turn, NOXs, both in normal tissue injuries and cancer.[26,28-30,68] Likewise, multiple MAPKs, including ERK1/2, AKT, JNK, and p38, seem to be oxidized by Mn porphyrins in tumor studies and subsequently inactivated.[28,69-71] For instance, MnE can suppress NOX4 upregulation (presumably via the NF-κB pathway) due to a radiation-induced increase in ROS levels.[72] MnBuOE reportedly activates Nrf2, presumably via oxidizing cysteines of Keap1, consequently upregulating endogenous antioxidative defenses.[73] Inhibition of these different mechanisms by Mn porphyrins would result in decreased ROS levels. Although the preferred mode of action of Mn porphyrins intracellularly is via suppression of NOXs,[15] or by directly targeting NF-κB and in turn inactivating NOXs, or activating Nrf2 by affecting Keap1, scavenging of ROS released outside the cells by these compounds cannot be excluded. In SCD, MnBuOE and MnE can treat an acute pain crisis by undoubtedly undergoing intricate interactions with numerous intracellular redox-sensitive pathways not only in SSRBCs by suppressing NOXs, MEK1/2, ERK1/2, and GRK2 signaling[15] but also in leukocytes and the endothelium,[28] pathways yet to be elucidated. Studies have shown that Mn porphyrins act both intracellularly (the cytosol, nucleus, and mitochondria) and extracellularly, mimicking extracellular SOD, MnSOD, and copper and zinc-containing SOD.[28,31,67,74] Furthermore, MnE and MnBuOE have a similar ability to interact with ROS.[31] However, their biodistribution is remarkably different due to a large, ~3.7 orders of magnitude difference in their lipophilicity.[31,38] Such a difference enables MnBuOE to distribute approximately threefold more in mitochondria than nucleus, whereas the mitochondria/nucleus ratio is 1.6 for MnE.[28] This could explain the increased efficiency of MnBuOE to reduce tissue oxidative stress observed in this study compared with MnE.

The wealth of the efficacy and toxicity data validated the progress of several Mn porphyrins toward multiple clinical trials.[59,67,75] Herein, we present the first report supporting the development of these Mn porphyrins, suppressors of at least SSRBC NOX-dependent ROS generation, as a safe subcutaneous therapy to reverse an acute vaso-occlusive crisis and prevent crisis establishment just when it begins in SCD. Thus, existing Mn porphyrins, including MnBuOE and MnE, warrant development as a first subcutaneous therapy for treating and relieving the progression of the pathognomonic acute vaso-occlusive episodes associated with SCD. Importantly, one should be mindful and cautious about the prophylactic use of these Mn porphyrins as a preventive treatment of inflammation-initiated

Figure 6. (continued) fields): kidneys (A), liver (B), and spleen (C) collected from treated TS mice (n = 4 per treatment condition) stained for ROS with DCF. Graphs show mean fluorescence (±SEM) of data for each organ collected from treated mice; $P < .05$ for Mn porphyrin–treated vs vehicle-treated (within an organ). (D-F) Mn porphyrin–modulated mRNA expression of ICAM-1 (D), VCAM-1 (E), and P-selectin (F) in tissue organs in TS mice. Relative quantification of mRNA expression (D-F) in the lungs, kidneys, liver, and spleen are presented as the mean ± SEM (n = 4 per organ/treatment condition). (G-J) Western blot analysis shows downregulation of ICAM-1, VCAM-1, and P-selectin expression in the lungs and/or kidneys. Data are presented as the mean ± SEM (n = 6-9 per organ/treatment condition). *$P < .05$, **$P < .01$, ***$P < .001$, and ****$P < .0001$ vs vehicle treatment. GAPDH, glyceraldehyde-3-phosphate dehydrogenase.

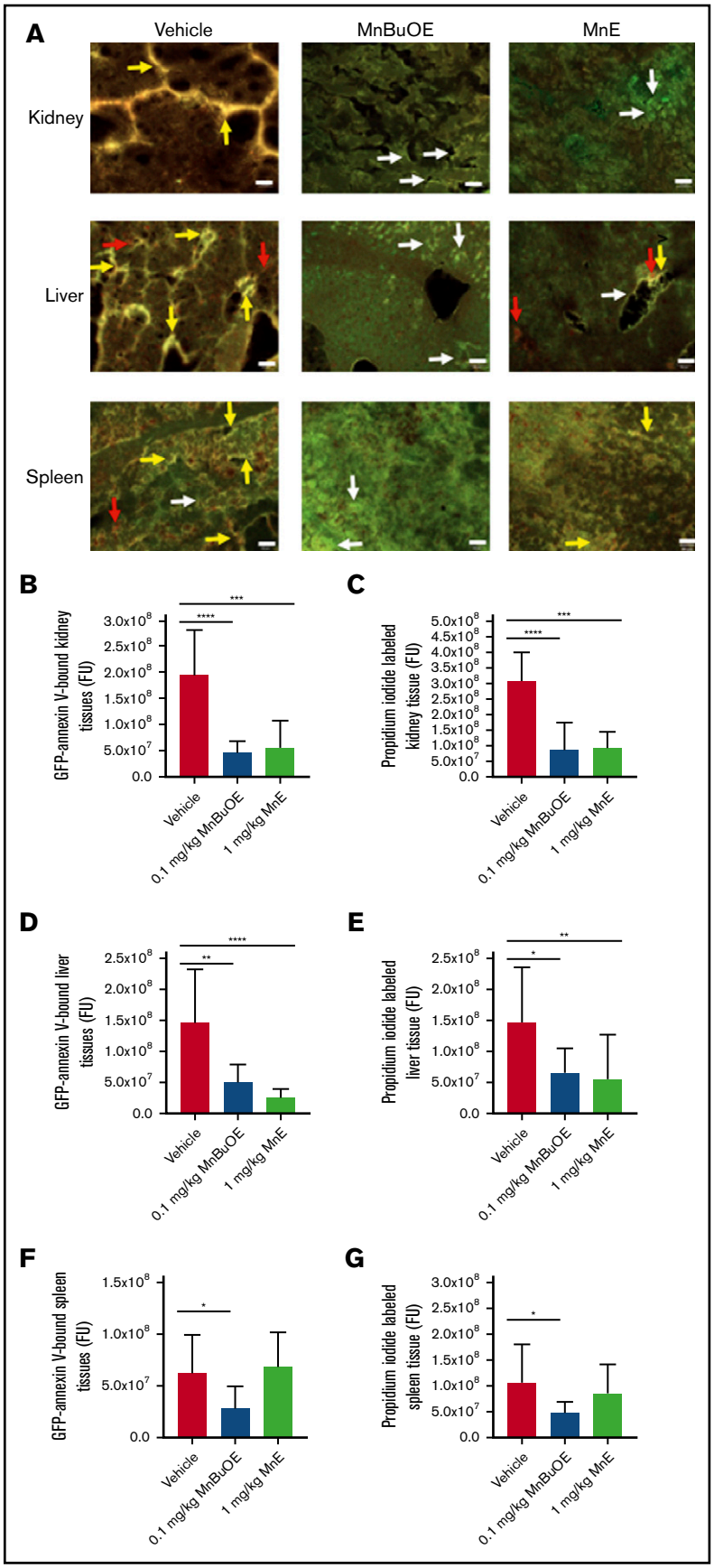

Figure 7. Mn porphyrins improve organ cell apoptosis in TS mice in vivo. (A) Representative dual-labeling studies with GFP-labeled annexin V and PI of tissue organs: kidneys, liver, and spleen isolated from TS mice treated with vehicle, 0.1 mg/kg MnBuOE, and 1 mg/kg MnE. GFP-labeled annexin V–binding (green color), PI-staining (red color), and double-staining (yellow or brown color) regions are indicated with arrows (white, red, and yellow arrows, respectively). Scale bars, 50 μm. (B-G) Separate quantitation of GFP (B,D,F) and PI (C,E,G) staining in each organ: kidneys (B-C), liver (D-E), and spleen (F -G) collected from treated TS mice. Mn porphyrins could indeed alleviate organ damage as reflected by decreased apoptosis compared with the vehicle group. Data are presented as the mean of n = 5 random fields/organ/treatment condition ± SEM (n = 4 animals per treatment condition). *$P < .05$, **$P < .01$, ***$P < .001$, and ****$P < .0001$ vs vehicle treatment. FU, fluorescence unit.

pain crises in SCD and/or pain crises caused by noninflammatory stimuli, such as exercise, even if a prolonged use of these agents might not cause a negative response in sickle mice.

Acknowledgment

This work was supported by the National Heart, Lung, and Blood Institute, National Institutes of Health (R01 HL137930) (R.Z.).

Authorship

Contribution: M.T., R.E., and R.Z. performed experiments related to the study, and M.T. helped quantifying in vivo data; I.B.-H. designed, synthesized, and provided the Mn porphyrins, helped with the animal treatment conditions of the studies related to Mn porphyrins, and edited the manuscript; and R.Z. planned the project, designed and supervised all of the research study, quantified, analyzed, interpreted and critiqued the data, and drafted the manuscript.

Conflict-of-interest disclosure: I.B.-H. is a consultant with BioMimetix JVLLC and holds equities in BioMimetix JVLLC. I.B.-H. and Duke University have patent rights and have licensed technologies to BioMimetix JVLLC. The remaining authors declare no competing financial interests.

ORCID profiles: M.T., 0000-0003-3740-0852; R.Z., 0000-0002-8220-3260.

Correspondence: Rahima Zennadi, Division of Hematology, Duke Comprehensive Sickle Cell Center, Department of Medicine, Duke University Medical Center, 203 Research Dr, Durham, NC 27710; e-mail: zenna001@mc.duke.edu.

References

1. Kaul DK, Tsai HM, Liu XD, Nakada MT, Nagel RL, Coller BS. Monoclonal antibodies to alphaVbeta3 (7E3 and LM609) inhibit sickle red blood cell-endothelium interactions induced by platelet-activating factor. *Blood*. 2000;95(2):368-374.
2. Hebbel RP, Yamada O, Moldow CF, Jacob HS, White JG, Eaton JW. Abnormal adherence of sickle erythrocytes to cultured vascular endothelium: possible mechanism for microvascular occlusion in sickle cell disease. *J Clin Invest*. 1980;65(1):154-160.
3. Zennadi R, Hines PC, De Castro LM, Cartron JP, Parise LV, Telen MJ. Epinephrine acts through erythroid signaling pathways to activate sickle cell adhesion to endothelium via LW-alphavbeta3 interactions. *Blood*. 2004;104(12):3774-3781.
4. De Castro LM, Zennadi R, Jonassaint JC, Batchvarova M, Telen MJ. Effect of propranolol as antiadhesive therapy in sickle cell disease. *Clin Transl Sci*. 2012;5(6):437-444.
5. Hebbel RP, Boogaerts MA, Eaton JW, Steinberg MH. Erythrocyte adherence to endothelium in sickle-cell anemia. A possible determinant of disease severity. *N Engl J Med*. 1980;302(18):992-995.
6. Solovey AA, Solovey AN, Harkness J, Hebbel RP. Modulation of endothelial cell activation in sickle cell disease: a pilot study. *Blood*. 2001;97(7):1937-1941.
7. Hebbel RP. Adhesion of sickle red cells to endothelium: myths and future directions. *Transfus Clin Biol*. 2008;15(1-2):14-18.
8. Siciliano A, Malpeli G, Platt OS, et al. Abnormal modulation of cell protective systems in response to ischemic/reperfusion injury is important in the development of mouse sickle cell hepatopathy. *Haematologica*. 2011;96(1):24-32.
9. Sabaa N, de Franceschi L, Bonnin P, et al. Endothelin receptor antagonism prevents hypoxia-induced mortality and morbidity in a mouse model of sickle-cell disease. *J Clin Invest*. 2008;118(5):1924-1933.
10. Mahaseth H, Vercellotti GM, Welch TE, et al. Polynitroxyl albumin inhibits inflammation and vasoocclusion in transgenic sickle mice. *J Lab Clin Med*. 2005;145(4):204-211.
11. Kaul DK, Liu XD, Zhang X, Ma L, Hsia CJ, Nagel RL. Inhibition of sickle red cell adhesion and vasoocclusion in the microcirculation by antioxidants. *Am J Physiol Heart Circ Physiol*. 2006;291(1):H167-H175.
12. Belcher JD, Chen C, Nguyen J, et al. Control of oxidative stress and inflammation in sickle cell disease with the Nrf2 activator dimethyl fumarate. *Antioxid Redox Signal*. 2017;26(14):748-762.
13. George A, Pushkaran S, Konstantinidis DG, et al. Erythrocyte NADPH oxidase activity modulated by Rac GTPases, PKC, and plasma cytokines contributes to oxidative stress in sickle cell disease. *Blood*. 2013;121(11):2099-2107.
14. Hebbel RP, Morgan WT, Eaton JW, Hedlund BE. Accelerated autoxidation and heme loss due to instability of sickle hemoglobin. *Proc Natl Acad Sci U S A*. 1988;85(1):237-241.
15. MacKinney A, Woska E, Spasojevic I, Batinic-Haberle I, Zennadi R. Disrupting the vicious cycle created by NOX activation in sickle erythrocytes exposed to hypoxia/reoxygenation prevents adhesion and vasoocclusion. *Redox Biol*. 2019;25:101097.
16. Kuypers FA, Scott MD, Schott MA, Lubin B, Chiu DTY. Use of ektacytometry to determine red cell susceptibility to oxidative stress. *J Lab Clin Med*. 1990;116(4):535-545.
17. Wood KC, Hebbel RP, Granger DN. Endothelial cell NADPH oxidase mediates the cerebral microvascular dysfunction in sickle cell transgenic mice. *FASEB J*. 2005;19(8):989-991.
18. Aslan M, Canatan D. Modulation of redox pathways in neutrophils from sickle cell disease patients. *Exp Hematol*. 2008;36(11):1535-1544.
19. Aslan M, Ryan TM, Adler B, et al. Oxygen radical inhibition of nitric oxide-dependent vascular function in sickle cell disease. *Proc Natl Acad Sci U S A*. 2001;98(26):15215-15220.
20. Kiefmann R, Rifkind JM, Nagababu E, Bhattacharya J. Red blood cells induce hypoxic lung inflammation. *Blood*. 2008;111(10):5205-5214.

21. Nur E, Biemond BJ, Otten HM, Brandjes DP, Schnog JJ, Group CS; CURAMA Study Group. Oxidative stress in sickle cell disease; pathophysiology and potential implications for disease management. *Am J Hematol*. 2011;86(6):484-489.

22. Nur E, Brandjes DP, Teerlink T, et al; CURAMA study group. N-acetylcysteine reduces oxidative stress in sickle cell patients. *Ann Hematol*. 2012;91(7):1097-1105.

23. Muskiet FA, Muskiet FD, Meiborg G, Schermer JG. Supplementation of patients with homozygous sickle cell disease with zinc, alpha-tocopherol, vitamin C, soybean oil, and fish oil. *Am J Clin Nutr*. 1991;54(4):736-744.

24. Dorai T, Fishman AI, Ding C, Batinic-Haberle I, Goldfarb DS, Grasso M. Amelioration of renal ischemia-reperfusion injury with a novel protective cocktail. *J Urol*. 2011;186(6):2448-2454.

25. Celic T, Španjol J, Bobinac M, et al. Mn porphyrin-based SOD mimic, MnTnHex-2-PyP(5+), and non-SOD mimic, MnTBAP(3-), suppressed rat spinal cord ischemia/reperfusion injury via NF-κB pathways. *Free Radic Res*. 2014;48(12):1426-1442.

26. Sheng H, Spasojevic I, Tse HM, et al. Neuroprotective efficacy from a lipophilic redox-modulating Mn(III) N-hexylpyridylporphyrin, MnTnHex-2-PyP: rodent models of ischemic stroke and subarachnoid hemorrhage. *J Pharmacol Exp Ther*. 2011;338(3):906-916.

27. Saba H, Batinic-Haberle I, Munusamy S, et al. Manganese porphyrin reduces renal injury and mitochondrial damage during ischemia/reperfusion. *Free Radic Biol Med*. 2007;42(10):1571-1578.

28. Batinic-Haberle I, Tovmasyan A, Spasojevic I. Mn porphyrin-based redox-active drugs: differential effects as cancer therapeutics and protectors of normal tissue against oxidative injury. *Antioxid Redox Signal*. 2018;29(16):1691-1724.

29. Jaramillo MC, Briehl MM, Batinic-Haberle I, Tome ME. Manganese (III) meso-tetrakis N-ethylpyridinium-2-yl porphyrin acts as a pro-oxidant to inhibit electron transport chain proteins, modulate bioenergetics, and enhance the response to chemotherapy in lymphoma cells. *Free Radic Biol Med*. 2015;83:89-100.

30. Jaramillo MC, Briehl MM, Crapo JD, Batinic-Haberle I, Tome ME. Manganese porphyrin, MnTE-2-PyP5+, acts as a pro-oxidant to potentiate glucocorticoid-induced apoptosis in lymphoma cells. *Free Radic Biol Med*. 2012;52(8):1272-1284.

31. Batinic-Haberle I, Tovmasyan A, Roberts ER, Vujaskovic Z, Leong KW, Spasojevic I. SOD therapeutics: latest insights into their structure-activity relationships and impact on the cellular redox-based signaling pathways. *Antioxid Redox Signal*. 2014;20(15):2372-2415.

32. Levasseur DN, Ryan TM, Pawlik KM, Townes TM. Correction of a mouse model of sickle cell disease: lentiviral/antisickling beta-globin gene transduction of unmobilized, purified hematopoietic stem cells. *Blood*. 2003;102(13):4312-4319.

33. Townes TM, Ryan TM, Behringer RR, Palmiter RD, Brinster RL. DNase I super-hypersensitive sites direct high level erythroid expression of human alpha-, beta- and beta s- globin genes in transgenic mice. *Prog Clin Biol Res*. 1989;316A:47-61.

34. Ryan TM, Townes TM, Reilly MP, et al. Human sickle hemoglobin in transgenic mice. *Science*. 1990;247(4942):566-568.

35. Chantrathammachart P, Mackman N, Sparkenbaugh E, et al. Tissue factor promotes activation of coagulation and inflammation in a mouse model of sickle cell disease. *Blood*. 2012;120(3):636-646.

36. Zennadi R, Moeller BJ, Whalen EJ, et al. Epinephrine-induced activation of LW-mediated sickle cell adhesion and vaso-occlusion in vivo. *Blood*. 2007;110(7):2708-2717.

37. Batinic-Haberle I, Benov L, Fridovich I. An anionic impurity in preparations of cytochrome c interferes with assays of cationic catalysts of the dismutation of the superoxide anion radical. *Anal Biochem*. 1999;275(2):267.

38. Rajic Z, Tovmasyan A, Spasojevic I, et al. A new SOD mimic, Mn(III) ortho N-butoxyethylpyridylporphyrin, combines superb potency and lipophilicity with low toxicity. *Free Radic Biol Med*. 2012;52(9):1828-1834.

39. Towbin H, Staehelin T, Gordon J. Electrophoretic transfer of proteins from polyacrylamide gels to nitrocellulose sheets: procedure and some applications. *Proc Natl Acad Sci USA*. 1979;76(9):4350-4354.

40. Hebbel RP, Osarogiagbon R, Kaul D. The endothelial biology of sickle cell disease: inflammation and a chronic vasculopathy. *Microcirculation*. 2004;11(2):129-151.

41. Turhan A, Weiss LA, Mohandas N, Coller BS, Frenette PS. Primary role for adherent leukocytes in sickle cell vascular occlusion: a new paradigm. *Proc Natl Acad Sci U S A*. 2002;99(5):3047-3051.

42. Butcher EC. Leukocyte-endothelial cell recognition: three (or more) steps to specificity and diversity. *Cell*. 1991;67(6):1033-1036.

43. Springer TA. Traffic signals for lymphocyte recirculation and leukocyte emigration: the multistep paradigm. *Cell*. 1994;76(2):301-314.

44. Wun T. The role of inflammation and leukocytes in the pathogenesis of sickle cell disease; haemoglobinopathy. *Hematology*. 2001;5(5):403-412.

45. Emokpae MA, Uadia PO, Gadzama AA. Correlation of oxidative stress and inflammatory markers with the severity of sickle cell nephropathy. *Ann Afr Med*. 2010;9(3):141-146.

46. Belcher JD, Mahaseth H, Welch TE, Otterbein LE, Hebbel RP, Vercellotti GM. Heme oxygenase-1 is a modulator of inflammation and vaso-occlusion in transgenic sickle mice. *J Clin Invest*. 2006;116(3):808-816.

47. Beckman JD, Belcher JD, Vineyard JV, et al. Inhaled carbon monoxide reduces leukocytosis in a murine model of sickle cell disease. *Am J Physiol Heart Circ Physiol*. 2009;297(4):H1243-H1253.

48. Makis AC, Hatzimichael EC, Stebbing J, Bourantas KL. C-reactive protein and vascular cell adhesion molecule-1 as markers of severity in sickle cell disease. *Arch Intern Med*. 2006;166(3):366-368.

49. Duits AJ, Pieters RC, Saleh AW, et al. Enhanced levels of soluble VCAM-1 in sickle cell patients and their specific increment during vasoocclusive crisis. *Clin Immunol Immunopathol*. 1996;81(1):96-98.

50. Al Najjar S, Adam S, Ahmed N, Qari M. Markers of endothelial dysfunction and leucocyte activation in Saudi and non-Saudi haplotypes of sickle cell disease. *Ann Hematol*. 2017;96(1):141-146.

51. Lancelot M, White J, Sarnaik S, Hines P. Low molecular weight heparin inhibits sickle erythrocyte adhesion to VCAM-1 through VLA-4 blockade in a standardized microfluidic flow adhesion assay. *Br J Haematol*. 2017;178(3):479-481.

52. White J, Krishnamoorthy S, Gupta D, et al. VLA-4 blockade by natalizumab inhibits sickle reticulocyte and leucocyte adhesion during simulated blood flow. *Br J Haematol*. 2016;174(6):970-982.

53. Luo W, Campbell A, Wang H, et al. P-selectin glycoprotein ligand-1 inhibition blocks increased leukocyte-endothelial interactions associated with sickle cell disease in mice. *Blood*. 2012;120(18):3862-3864.

54. Gutsaeva DR, Parkerson JB, Yerigenahally SD, et al. Inhibition of cell adhesion by anti-P-selectin aptamer: a new potential therapeutic agent for sickle cell disease. *Blood*. 2011;117(2):727-735.

55. Nath KA, Grande JP, Haggard JJ, et al. Oxidative stress and induction of heme oxygenase-1 in the kidney in sickle cell disease. *Am J Pathol*. 2001;158(3): 893-903.

56. Kaul DK, Liu XD, Choong S, Belcher JD, Vercellotti GM, Hebbel RP. Anti-inflammatory therapy ameliorates leukocyte adhesion and microvascular flow abnormalities in transgenic sickle mice. *Am J Physiol Heart Circ Physiol*. 2004;287(1):H293-H301.

57. Paloschi MV, Boeno CN, Lopes JA, et al. Role of l-amino acid oxidase isolated from Calloselasma rhodostoma venom on neutrophil NADPH oxidase complex activation. *Toxicon*. 2018;145:48-55.

58. Tumurkhuu G, Koide N, Dagvadorj J, et al. MnTBAP, a synthetic metalloporphyrin, inhibits production of tumor necrosis factor-alpha in lipopolysaccharide-stimulated RAW 264.7 macrophages cells via inhibiting oxidative stress-mediating p38 and SAPK/JNK signaling. *FEMS Immunol Med Microbiol*. 2007;49(2):304-311.

59. Bruni A, Pepper AR, Gala-Lopez B, et al. A novel redox-active metalloporphyrin reduces reactive oxygen species and inflammatory markers but does not improve marginal mass engraftment in a murine donation after circulatory death islet transplantation model. *Islets*. 2016;8(4):e1190058.

60. Regan-Komito D, Swann JW, Demetriou P, et al. GM-CSF drives dysregulated hematopoietic stem cell activity and pathogenic extramedullary myelopoiesis in experimental spondyloarthritis. *Nat Commun*. 2020;11(1):155.

61. Jahandideh B, Derakhshani M, Abbaszadeh H, et al. The pro-Inflammatory cytokines effects on mobilization, self-renewal and differentiation of hematopoietic stem cells. *Hum Immunol*. 2020;81(5):206-217.

62. Schaer DJ, Buehler PW, Alayash AI, Belcher JD, Vercellotti GM. Hemolysis and free hemoglobin revisited: exploring hemoglobin and hemin scavengers as a novel class of therapeutic proteins. *Blood*. 2013;121(8):1276-1284.

63. Wagener FA, Eggert A, Boerman OC, et al. Heme is a potent inducer of inflammation in mice and is counteracted by heme oxygenase. *Blood*. 2001; 98(6):1802-1811.

64. Wagener FA, Abraham NG, van Kooyk Y, de Witte T, Figdor CG. Heme-induced cell adhesion in the pathogenesis of sickle-cell disease and inflammation. *Trends Pharmacol Sci*. 2001;22(2):52-54.

65. Rother RP, Bell L, Hillmen P, Gladwin MT. The clinical sequelae of intravascular hemolysis and extracellular plasma hemoglobin: a novel mechanism of human disease. *JAMA*. 2005;293(13):1653-1662.

66. Tovmasyan A, Sampaio RS, Boss MK, et al. Anticancer therapeutic potential of Mn porphyrin/ascorbate system. *Free Radic Biol Med*. 2015;89: 1231-1247.

67. Batinic-Haberle I, Tome ME. Thiol regulation by Mn porphyrins, commonly known as SOD mimics. *Redox Biol*. 2019;25:101139.

68. Sheng H, Yang W, Fukuda S, et al. Long-term neuroprotection from a potent redox-modulating metalloporphyrin in the rat. *Free Radic Biol Med*. 2009; 47(7):917-923.

69. Evans MK, Tovmasyan A, Batinic-Haberle I, Devi GR. Mn porphyrin in combination with ascorbate acts as a pro-oxidant and mediates caspase-independent cancer cell death. *Free Radic Biol Med*. 2014;68:302-314.

70. Shin SW, Choi C, Lee GH, et al. Mechanism of the antitumor and radiosensitizing effects of a manganese porphyrin, MnHex-2-PyP. *Antioxid Redox Signal*. 2017;27(14):1067-1082.

71. Tovmasyan A, Bueno-Janice JC, Jaramillo MC, et al. Radiation-mediated tumor growth inhibition is significantly enhanced with redox-active compounds that cycle with ascorbate. *Antioxid Redox Signal*. 2018;29(13):1196-1214.

72. Pazhanisamy SK, Li H, Wang Y, Batinic-Haberle I, Zhou D. NADPH oxidase inhibition attenuates total body irradiation-induced haematopoietic genomic instability. *Mutagenesis*. 2011;26(3):431-435.

73. Zhao Y, Carroll DW, You Y, et al. A novel redox regulator, MnTnBuOE-2-PyP^{5+}, enhances normal hematopoietic stem/progenitor cell function. *Redox Biol*. 2017;12:129-138.

74. Batinić-Haberle I, Rebouças JS, Spasojević I. Superoxide dismutase mimics: chemistry, pharmacology, and therapeutic potential. *Antioxid Redox Signal*. 2010;13(6):877-918.

75. Bruni A, Pepper AR, Pawlick RL, et al. BMX-001, a novel redox-active metalloporphyrin, improves islet function and engraftment in a murine transplant model. *Am J Transplant*. 2018;18(8):1879-1889.